Micrometer x-ray diffraction study of VO_2 films: Separation between metal-insulator transition and structural phase transition

Bong-Jun Kim,* Yong Wook Lee, Sungyeoul Choi, Jung-Wook Lim, Sun Jin Yun, and Hyun-Tak Kim†
Metal-Insulator Transition device Team, Electronic and Telecommunications Research Institute, Daejeon 305-350, Korea

Tae-Ju Shin and Hwa-Sick Yun
Pohang Accelerator Laboratory, Pohang University of Science and Technology, Pohang 790-784, Korea
(Received 21 April 2008; published 2 June 2008)

In order to clarify whether VO_2 is a Mott insulator or a Peierls insulator, the metal-insulator transition (MIT) and the structural phase transition (SPT) are simultaneously monitored for VO_2 films by current-voltage curve and diffraction measurements using a synchrotron micro-x-ray beam. In the regime showing a metallic conductivity below the SPT temperature (approximately 70 °C), only the diffraction planes of the monoclinic structure are observed, while planes of the tetragonal structure are absent. This observation reveals the presence of a monoclinic and metal phase between the MIT and the SPT as a characteristic of a Mott insulator.

DOI: 10.1103/PhysRevB.77.235401 PACS number(s): 71.27.+a, 68.37.Yz, 71.30.+h

I. INTRODUCTION

Recently, many researchers have paid attention to the mechanism of the long issued Mott metal-insulator transition (MIT) to clarify phenomena such as high-T_c superconductivity and colossal magnetoresistance,[1] as well as MIT devices, using the current jump for overcoming limitations of semiconductor devices such as power transistors[1,2] and nonvolatile memory.[3] Since the current jump was also suggested as the Mott MIT,[1] it needs to be clearly explained.

A representative material, VO_2 (half-filled V^{4+}, $3d^1$), with a metallic electronic structure shows an abrupt resistance change as the MIT and the structural phase transition (SPT) between the monoclinic (M) and the rutile (R) tetragonal structures near 70 °C. In fact, researchers have been long arguing whether VO_2 is a Mott insulator or a Peierls insulator.[4,5] A Mott insulator undergoes a first-order MIT via the breakdown of a strongly correlated critical electron-electron Coulomb interaction without a SPT.[6,7] When VO_2 was thought of as a Mott insulator, it was known as the monoclinic M_2 insulator consisting of equally spaced V chains.[4,8] However, for a Peierls insulator, it has been proposed that VO_2 has the d_{II}-bonding combination of $3d^1$ electrons.[9]

A Peierls insulator is caused by electron-phonon interaction such as a charge-density wave.[10] The Peierls MIT is then accompanied by a SPT, i.e., the MIT and the SPT occur simultaneously without the first-order MIT. An orbital-assisted MIT model,[11] a structure-driven MIT,[12] and an ultrafast decrease of the transmittance within 0.7 ps[13] proposed the Peierls picture without simultaneous measurements of two transitions.

Furthermore, for explaining the transition from the monoclinic M_1 phase to the R metal phase, suggestions including electron-electron interaction and electron-phonon interaction were reported.[14–16] A carrier generation caused by a shift of the d band to the Fermi surface was observed by photoemission spectroscopy.[15,17,18]

From optical studies, a diverging effective mass has been inferred as evidence of a correlated system undergoing the Mott MIT.[19] A monoclinic and correlated metal (MCM) phase in VO_2 was measured by observations of coherent phonons using the femtosecond pump-probe technique[20] and optical phonons using micro-Raman scattering[1] at high pressures.[21] The MCM phase was also observed by current-voltage measurements.[22] In addition, the M structure was observed at the transition region where resistance abruptly dropped.[23,24]

The above controversial argument arises from a preconception that the MIT and the SPT occur simultaneously and from component inhomogeneity in VO_2 samples. The component inhomogeneity generates temperature inhomogeneity between grains near $T_{\text{SPT}} \approx 70$ °C; finally, this induces a structural inhomogeneity. This structural inhomogeneity indicates a mixing of both the M structure of the low-temperature insulating phase and the R structure of the high-temperature metallic phase even below T_{SPT}.[25,26] Thus, a direct observation of the monoclinic and metal phase using a micro-x-ray beam has become imperative to settle this argument.

In this paper, we report both the temperature dependence of the SPT using a polychromatic synchrotron micro-x-ray beam for a VO_2 film and the observation of the monoclinic and metal phase by simultaneous measurements of the MIT and the SPT for a VO_2-based two-terminal device. Furthermore, the absence of the structural inhomogeneity is revealed.

II. EXPERIMENT

VO_2 thin films on (1010) Al_2O_3 substrates were prepared by a pulsed laser deposition method described in a previous paper.[27] The thickness of the films was approximately 100 nm. For observing the temperature dependence of the SPT, a VO_2 thin film of 1×1 cm^2 was used. For measurements of the voltage dependence of the MIT, a VO_2-based two-terminal device was fabricated (inset of Fig. 3). The VO_2 film in the device was patterned by Ar^+ ion-milling. Nickel electrodes were deposited for ohmic contact. The device had a channel width of 3 μm and a channel length of 10 μm.

 ©2008 The American Physical Society

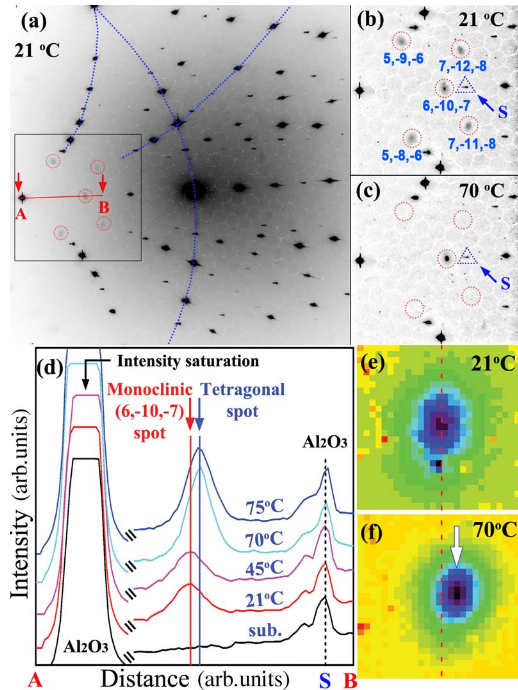

FIG. 1. (Color online) (a) Laue spots measured at 21 °C by a micro-x-ray beam. Strong spots are from the $(10\bar{1}0)$ Al_2O_3 substrate, and the weak spots in the box come from the VO_2 film. (b) An enlarged image of the box in Fig. 1(a). VO_2 spots circled by red dots are indexed. The reference Al_2O_3 spot is denoted by *S*. (c) An enlarged image of the VO_2 spot measured at 70 °C. (d) Scanned intensity taken from A to B in the box of Fig. 1(a). A strong spot near A is one of the substrate spots and a weak spot near B is one of the center spots coming from the VO_2 film. The reference Al_2O_3 spots do not move with temperature. (e) Enlarged image of the center spot, (6,−10,−7), in the monoclinic structure at 21 °C. (f) Enlarged image of the center spot in the tetragonal structure at 70 °C. The position difference between two center spots is shown in Figs. 1(e) and 1(f).

The device was intentionally manufactured to have a large leakage current (current near zero voltage in Fig. 3) and a small current jump in order to avoid breakdown (conducting path) by high current and static electricity on the basis of previous results.[1–3,22] The resistance ratio of the transition between points E and F in Fig. 3 was estimated as approximately 70, considerably less than $\sim 10^3$ for a good film; this indicates that the film is leaky. Note that a device with a large current jump had a conducting path in a high current. For easy beam alignment, a long Ni line of 0.35 mm between the electrode pads and the film (inset of Fig. 3) was patterned. Current-voltage, *I*-*V*, characteristics for the device were measured by a precision semiconductor parameter analyzer (HP4156C).

We used the focused polychromatic synchrotron micro-x-ray beam in the 1B2 beam line at the Pohang Accelerator Laboratory for structure analysis of the VO_2 films as a function of temperature and voltage. The experiments were carried out twice due to the limitation of beam time. Figure 1 was measured at the first beam time. Figures 3 and 4 were observed after awaiting six months to obtain another beam time. After a beam alignment using a 5 mm thick Ge single crystal, a polychromatic micro-x-ray beam with a spot size of 3×2.5 μm^2 was focused on the channel of the VO_2 films using a pair of mirrors in a Kirkpatrick-Baez configuration.[28] Laue patterns of VO_2 with temperature and voltage were taken by a charge coupled device (CCD) camera (1340 $\times$1300 pixels, Roper Scientific, Inc.). Each Laue pattern was recorded for 60 s. For the intensification of the Laue pattern, several Laue patterns obtained under the same conditions were summed with an image tool at every measurement step.

III. RESULTS AND DISCUSSION

Figures 1(a)–1(c) show the temperature dependence of the micro-x-ray diffraction patterns for a VO_2 film. Spots in the patterns are due to planes diffracted from the 3×2.5 μm^2 area on VO_2/Al_2O_3 by the focused polychromatic micro-x-ray beam. The strong Laue spots in Fig. 1(a) are those of the substrate, while the weak Laue spots denoted by red circles in the guided box are from the VO_2 film. For close examination of the weak Laue spots, the image in the box of Fig. 1(a) is enlarged and sharpened by image processing tools, as shown in Fig. 1(b). Five Laue spots indicated by red-dot circles are planes corresponding to the monoclinic structure in VO_2; the plane indices are written in the figure. These weak M Laue spots disappear at 70 °C leaving only the center spot, as shown in Fig. 1(c). A plane index of the center spot at 70 °C is not determined using only one spot in the simulation program, but the center spot is regarded as a plane in the tetragonal structure on the basis of previous measurements.[12,22,24]

In order to observe whether there is the shift of the center spots in the M and R structures, we scanned the position of the spots from A to B in the box of Fig. 1(a) with temperature, as shown in Fig. 1(d). Reference Al_2O_3 spots indicated by mark S in Fig. 1(d) do not move with temperature. A new peak in the tetragonal structure appears at a position slightly shifted to the right from (6,−10,−7) the M peak. Spot images indicating the different positions of the center spots are shown in Figs. 1(e) and 1(f). Thus, the disappearance of the five diffraction spots and the emergence of one strong spot in the center indicate that VO_2 underwent a SPT from the M to the tetragonal structure.

The above Laue spot indices and information on the structural alignment in VO_2/Al_2O_3 were obtained by analyzing the data with a simulation program.[29] In the real configuration of the measurement, the polychromatic x-ray beam along the $-z$ direction was focused on the tilted sample plane and the Laue patterns were collected with the CCD camera. In the simulation program, a back-reflection method was selected and the simulation parameters in the Fig. 2(b) caption were determined to have the same Laue pattern [Fig. 1(a)]. Figure 2(a) shows a diagram of the structure resulting from the simulation configuration with the crystal alignment information. The VO_2 film deposited on the (1010) Al_2O_3 substrate has a tilted (011) plane of 37° to the substrate plane. The normal crystal directions (y direction) of VO_2 and Al_2O_3 to the incident x ray are $[\bar{2}10]$ and $[1\bar{1}0]$, respectively. Figure 2(b) shows the Laue pattern simulated by using these parameters in VO_2. Figure 2(c) exhibits that the boxed area in Fig.

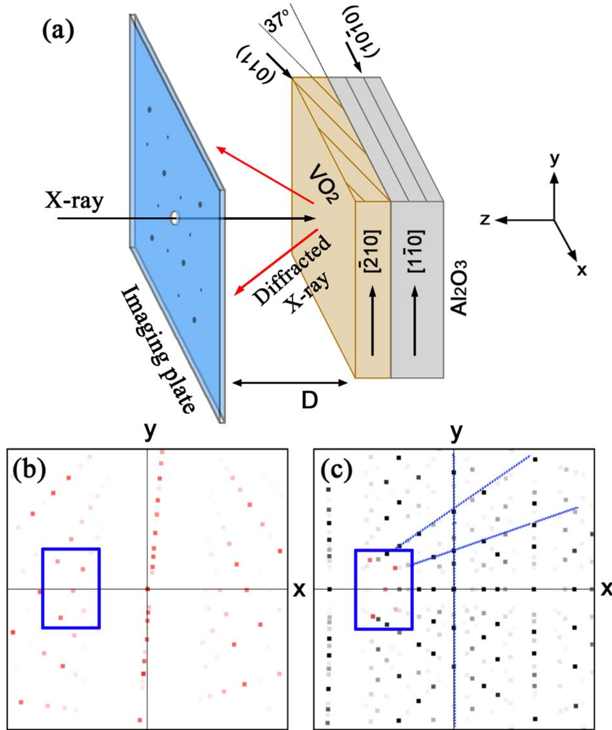

FIG. 2. (a) (Color online) A schematic diagram of the simulation configuration of x-ray microdiffraction. (b) A computer-calculated Laue pattern of a tilted (011) VO_2 plane with a 37° slope along the x axis. The vertical y direction is [$\bar{2}$10]. Spots in the blue boxed area are similar to those in the box of Fig. 1(a). The simulation parameters of VO_2, a=5.7520 Å, b=4.5380 Å, and c=5.3830 Å, a monoclinic angle of β=122.60°, and space group P121/c 1(14)-monoclinic were used. (c) A computer-calculated Laue pattern of the (10$\bar{1}$0) Al_2O_3 substrate with a [1$\bar{1}$0] vertical direction to the y axis. The only blue boxed area in (b) overlaps the simulated Al_2O_3 Laue pattern to compare with the true image of Fig. 1(a).

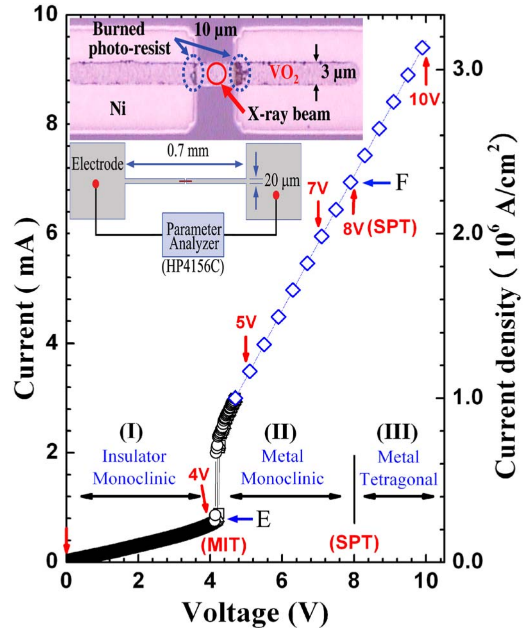

FIG. 3. (Color online) Inset: A microsurface image of the device with a length of 10 μm and a width of 3 μm after finishing experiments. The micro-x-ray beam was focused on the center of the VO_2 film. The uniform black marks to the cross-sectional direction at both electrode sides translate to burned photoresists by high currents; this is evidence of the absence of the current path (breakdown). I-V sweeps for the device were simultaneously measured with micro-x-ray diffraction experiments. V_{MIT} is 4.2 V at the jump. The micro-x-ray measurements were carried out at voltages of 0, 4, 5, 7, 8, and 10 V.

2(b) overlaps the simulated Al_2O_3 Laue pattern at the same position. This area is included into the boxed area in Fig. 1(a).

Figure 3 shows the I-V curve observed for revealing the relation between the MIT and the SPT for the VO_2-based two-terminal device installed in the x-ray diffraction hutch. The MIT voltage is approximately 4.2 V. The ohmic behavior, corresponding to the characteristic of a metal, is observed above 4.2 V. This indicates that the VO_2 film became a metal. Furthermore, the current jump near 4.2 V was explained by the divergence in the hole-driven MIT theory [extended Brinkman-Rice[1,6,30] (BR) picture] and the BR picture.[7]

The image in the inset of Fig. 3, taken after finishing measurements, shows a device consisting of the etched VO_2 film on which the x-ray beam of 3×2.5 μm^2 was focused and exhibits black marks on both electrode sides. The black marks translate to residual photoresist (used for the lift-off process of a metal electrode) burned by high currents after the jump, and their shapes are uniform to the cross-sectional direction. This indicates that current uniformly flowed in the channel width. The maximum current during the experiment was as high as 25 mA. The device reproduced similar I-V characteristic curves to those obtained even after finishing x-ray diffraction experiments.

For the structural analysis of VO_2, each I-V measurement and the micro-x-ray experiment were simultaneously performed at each voltage. Laue patterns were obtained at several voltages. These measurement points are denoted by arrows in Fig. 3. During the measurement of each Laue pattern, a constant current was sustained.

Figures 4(a)–4(f) show the voltage dependence of micro-x-ray diffraction patterns measured for the device at room temperature. The micro-x-ray experiments were carried out at the voltage values indicated by the arrows in Fig. 3. The substrate Laue patterns are slightly different from that in Fig. 1(a) because of the difference of the experimental configuration. Five clear M VO_2 spots are shown from 0 to 5 V in Figs. 4(a)–4(c). At 7 and 8 V, the four spots excluding the central spot become very weak. At 10 V, only the center spot is very clear [Fig. 4(f)]. These results indicate that the M structure begins to change to the R structure from 8 V. The VO_2 film has the M structure up to 7 V, although the MIT at 4.2 V has already occurred (Fig. 3).

Figure 4(g) shows the intensity changes of five spots with increasing voltage. The remarkable decrease in the intensity of the P1, P2, P3, P4, and M spots are not observed up to 7 V. At 8 V and higher, the intensity of the M spot slightly increases because a new T spot appears, while other spots abruptly drop to zero. The intensities of the substrate spots

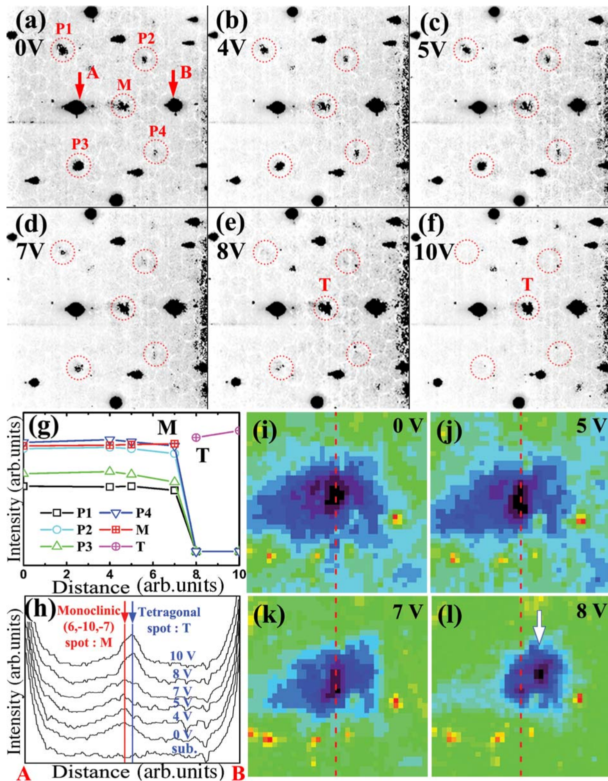

FIG. 4. (Color online) Voltage dependence of Laue patterns measured at voltage values denoted in Fig. 3. In (a)–(f), the strong Laue spots arise from the Al_2O_3 substrate, and weak spots come from the VO_2 film. (g) Intensity changes of P1, P2, P3, P4, M, and T spots denoted in (a)–(f) with increasing voltage to constant intensity of substrate spots. (h) A scanned image through the center spots from A to B as indicated in (a). (i)–(l) Enlarged images near the center spots. (k) and (l) show the positional difference between the center spots.

remained relatively constant. This indicates that the dominant structural change occurs between 7 and 8 V.

We can assume a structural inhomogeneity with both the M structure of a low temperature semiconducting phase and the R structure of a high-temperature metallic phase between 5 and 7 V. In this case, five Laue spots would be observed because the R structure has only one spot near $(6,-10,-7)$. Therefore, it is very important to find the positional difference between the center spots. A position near the center spot was scanned [Fig. 4(h)], and the scan data show broad peaks including the tetragonal center spot at 8 and 10 V. Splitting of the two spots is not obvious, and this can be attributed to background noise shown with blue color in Figs. 4(i)–4(l). The magnified spot images at 0, 5, and 7 V in Figs. 4(i)–4(k) exhibit only the M center spot of $(6,-10,-7)$. The spot image at 8 V in Fig. 4(l) displays the R tetragonal center spot, which is caused by a temperature increase induced by joule heating due to the high current; the temperature will be equal to or larger than T_{SPT}. This indicates that the metal phase in the VO_2 film has only an M structure between 4 and 7 V. The metallic phase from 4 to 7 V is regarded as the monoclinic metal (MM) phase (region II in Fig. 3).

The MM phase can be also regarded as the monoclinic and correlated metal (MCM) phase as evidence of the Mott MIT;[20,30] the presence of the correlation in the MM phase was deduced by the spectroscopic method in a previous paper.[19] The Mott MIT can be viewed as a transition between the M_2 antiferromagnetic insulator phase[4] and the MCM phase.

The MIT between the M insulator phase and the MM phase observed here differs from the MIT between the M_2 insulator phase and the R metal phase[4,8] and is also distinct from the MIT between the M_1 insulator phase and the R metal phase, as observed by many authors.[5,9,11–13] The absence of a strong correlation in the R metal phase was shown in the inset of Fig. 3(d) in Ref. 19.

IV. CONCLUSION

In conclusion, by observing the monoclinic and metal phase between the MIT and the SPT using a focused polychromatic synchrotron micro-x-ray beam, it is interpreted that VO_2 is a Mott insulator undergoing the first-order Mott MIT prior to SPT.

ACKNOWLEDGMENTS

We acknowledge D. N. Basov and M. M. Qazilbash for their valuable comments. This research was supported by the High-Risk High Return projects at ETRI.

*bjkim@etri.re.kr
†htkim@etri.re.kr

[1] H. T. Kim, B. G. Chae, D. H. Youn, S. L. Maeng, G. Kim, K. Y. Kang, and Y. S. Lim, New J. Phys. **6**, 52 (2004).
[2] J. S. Lee, M. Ortolani, U. Schade, Y. J. Chang, and T. W. Noh, Appl. Phys. Lett. **91**, 133509 (2007).
[3] M. Fiebig, K. Miyano, Y. Tomioka, and Y. Tokura, Science **280**, 1925 (1998).
[4] T. M. Rice, H. Launois, and J. P. Pouget, Phys. Rev. Lett. **73**, 3042 (1994).
[5] R. M. Wentzcovitch, W. W. Schulz, and P. B. Allen, Phys. Rev. Lett. **72**, 3389 (1994).
[6] H. T. Kim, Physica C **341-348**, 259 (2002); H. T. Kim, *New Trends in Superconductivity*, NATO Science Series, II/67 (Kluwer, Dordrecht, 2002), p. 137.
[7] W. F. Brinkman and T. M. Rice, Phys. Rev. B **2**, 4302 (1970).
[8] J. P. Pouget, H. Launois, J. P. D'Haenens, P. Merender, and T. M. Rice, Phys. Rev. Lett. **35**, 873 (1975).
[9] J. B. Goodenough, J. Solid State Chem. **5**, 145 (1972).
[10] J. B. Boyce, F. G. Bridges, T. Claeson, T. H. Geballe, G. G. Li, and A. W. Sleight, Phys. Rev. B **44**, 6961 (1991).
[11] M. W. Haverkort, Z. Hu, A. Tanaka, W. Reichelt, S. V. Streltsov, M. A. Korotin, V. I. Anisimov, H. H. Hsieh, H. J. Lin, C. T. Chen, D. I. Khomskii, and L. H. Tjeng, Phys. Rev. Lett. **95**,

196404 (2005).

[12] A. Cavalleri, Cs. Toth, C. W. Siders, J. A. Squier, F. Raksi, P. Forget, and J. C. Kieffer, Phys. Rev. Lett. **87**, 237401 (2001).

[13] M. Nakajima, N. Takubo, Z. Hiroi, Y. Ueda, and T. Suemoto, Appl. Phys. Lett. **92**, 011907 (2008).

[14] S. Biermann, A. Poteryaev, A. I. Lichtenstein, and A. Georges, Phys. Rev. Lett. **94**, 026404 (2005).

[15] K. Okazaki, H. Wadati, A. Fujimori, M. Onoda, Y. Muraoka, and Z. Hiroi, Phys. Rev. B **69**, 165104 (2004).

[16] C. Kübler, H. Ehrke, R. Huber, R. Lopez, A. Halabica, R. F. Haglund, Jr., and A. Leitenstorfer, Phys. Rev. Lett. **99**, 116401 (2007).

[17] R. Eguchi, M. Taguchi, M. Matsunami, K. Horiba, K. Yamamoto, Y. Ishida, A. Chainani, Y. Takata, M. Yabashi, D. Miwa, Y. Nishino, T. Tamasaku, T. Ishikawa, Y. Senba, H. Ohashi, Y. Muraoka, Z. Hiroi, and S. Shin, arXiv:cond-mat/0607712 (unpublished).

[18] M. Gatti, F. Bruneval, V. Olevano, and L. Reining, Phys. Rev. Lett. **99**, 266402 (2007).

[19] M. M. Qazilbash, M. Brehm, B. G. Chae, P. C. Ho, G. O. Andreev, B. J. Kim, S. J. Yun, A. V. Balatsky, M. B. Maple, F. Keilmann, H. T. Kim, and D. N. Bosov, Science **318**, 1750 (2007).

[20] H. T. Kim, Y. W. Lee, B. J. Kim, B. G. Chae, S. J. Yun, K. Y. Kang, K. J. Han, K. J. Yee, and Y. S. Lim, Phys. Rev. Lett. **97**, 266401 (2006).

[21] E. Arcangeletti, L. Baldassarre, D. Di Castro, S. Lupi, L. Malavasi, C. Marini, A. Perucchi, and P. Postorino, Phys. Rev. Lett. **98**, 196406 (2007).

[22] B. J. Kim, Y. W. Lee, B. G. Chae, S. J. Yun, S. Y. Oh, H. T. Kim, and Y. S. Lim, Appl. Phys. Lett. **90**, 023515 (2007).

[23] M. S. Grinolds, V. A. Lobastov, J. Weissenrieder, and A. H. Zewail, Proc. Natl. Acad. Sci. U.S.A. **103**, 18427 (2006).

[24] P. Baum, D. S. Yang, and A. H. Zewail, Science **318**, 788 (2007).

[25] H. S. Choi, J. S. Ahn, J. H. Jung, T. W. Noh, and D. H. Kim, Phys. Rev. B **54**, 4621 (1996).

[26] Y. J. Chang, J. S. Yang, Y. S. Kim, D. H. Kim, T. W. Noh, D.-W. Kim, E. Oh, B. Kahng, and J.-S. Chung, Phys. Rev. B **76**, 075118 (2007).

[27] B. J. Kim, Y. W. Lee, S. Choi, B. G. Chae, and H. T. Kim, J. Korean Phys. Soc. **50**, 653 (2007).

[28] J. S. Chung, H. S. Youn, and H. D. Joo, J. Korean Phys. Soc. **44**, 256 (2004).

[29] Download for free on http://ccp14.sims.nrc.ca/ccp/web-mirrors/xianrong-huang/.

[30] H. T. Kim, B. J. Kim, Y. W. Lee, B. G. Chae, and S. J. Yun, Physica B (Amsterdam) **403**, 1434 (2008).